AAC
Journals.ASM.org

Introduction of a Lysine Residue Promotes Aggregation of Temporin L in Lipopolysaccharides and Augmentation of Its Antiendotoxin Property

Saurabh Srivastava, Jimut Kanti Ghosh

Molecular and Structural Biology Division, CSIR-Central Drug Research Institute, Chattar Manzil Palace, Lucknow, India

Temporin L (TempL) is a 13-residue frog antimicrobial peptide that shows moderate bactericidal activity and antiendotoxin properties in macrophages. We envisioned that, due to its very hydrophobic nature, the peptide might fail to show its desired biological properties. It was predicted by employing the available algorithms that the replacement of a glutamine by lysine at position 3 could appreciably reduce its aggregation propensity in an aqueous environment. In order to investigate the structural, functional, and biological consequences of replacement of glutamine by lysine at its third position, TempL and the corresponding analog, Q3K-TempL, was synthesized and characterized. Introduction of the lysine residue significantly promoted the self-assembly and oligomeric state of TempL in lipopolysaccharide (LPS). Q3K-TempL exhibited augmented binding to LPS and also dissociated LPS aggregates with greater efficacy than TempL. Further, Q3K-TempL inhibited the LPS-induced proinflammatory cytokines in rat primary macrophages *in vitro* and *in vivo* in BALB/c mice with greater efficacy than TempL. The results showed that a simple amino acid substitution in a short hydrophobic antimicrobial peptide, TempL, enhanced its antiendotoxin properties and illustrate a plausible correlation between its aggregation properties in LPS and LPS detoxification activity.

Conventional antibiotics target important mechanisms or pathways of bacterial survival to inhibit their growth. However, failure of these conventional antibiotics to check the bacterial infections has been a major threat to human health in recent years due to the emergence of resistance in microbial organisms to these molecules. The inability of the conventional antibiotics to prevent unwanted stimulation of the host immune system by dead bacteria and their remains is also a serious disadvantage of their use. The toxins, such as bacterial-membrane constituents, nuclear materials, and cell debris, released by bacteria by means of cell division or after death can suddenly provoke the host immune system. Of these, lipopolysaccharide (LPS), also known as endotoxin, which is the main constituent of the outer membrane of Gram-negative bacteria, is a well-known activator of the humoral and cellular immune systems in the host and can produce serious pathophysiological consequences (1). Uncontrolled stimulation of the host immune system in the presence of LPS could result in excessive release of inflammatory cytokines, leading to septic shock, which often causes the death of a patient (2, 3). Septicemia is a leading cause of death that can be instigated even by ordinary Gram-negative bacterial infection. The neutralization of LPS-mediated toxic injury has been considered for a long time to be a possible therapeutic target in patients.

Antimicrobial peptides (AMPs) are important components of the innate immune system and have been identified in almost all living organisms, including humans (4). These small cationic polypeptides are capable of targeting bacteria, fungi, and enveloped viruses and are considered potential alternatives to conventional antibiotics. AMPs are mostly membrane active and lyse microbes by disintegrating their cell membranes, thus not giving them an opportunity to acquire resistance against the molecules (5). It is not only their mode of action that makes them better candidates for developing lead bactericidal molecules; their capabilities to bind and neutralize bacterial remains add to the advantages of antimicrobial peptides in their efficacy against bacterial invasion (6, 7). Not every antimicrobial peptide can neutralize proinflammatory responses stimulated by bacterial debris, principally LPS, but there are several AMPs that possess both bactericidal and antiendotoxin properties, and modulation of some parameters may enhance both biological properties in a peptide (8–10). LPS, present in the outer leaflet of the bacterial cell membrane, makes the outer membrane a highly asymmetric permeability barrier for the resistance of bacteria to external molecules, such as hydrophobic antibiotics, detergents, and other membrane-permeabilizing agents (11, 12).

Temporin L (TempL) is a 13-residue cationic antimicrobial peptide that possesses a wide spectrum of antimicrobial activities against Gram-negative and Gram-positive bacteria, as well as appreciable immunomodulatory properties against LPS-stimulated proinflammatory responses. Earlier work with Temporin L suggested that it is a self-aggregated antimicrobial peptide and that the self-aggregation behavior of the peptide is responsible for less solubility and less bioactivity than expected (13). The N terminus of Temporin L does not possess any cationic residues; by employing available algorithms, we found that replacement of glutamine with lysine at the third position of TempL could reduce its aggregation in an aqueous environment. The antibacterial properties of a Temporin L analog, (Arg^3)TL, with an arginine residue in place of glutamine at the number 3 position, has been reported recently

Received 5 February 2013 **Accepted** 4 March 2013
Published ahead of print 11 March 2013
Address correspondence to Jimut Kanti Ghosh, jighosh@yahoo.com.
This article is CSIR-CDRI Communication number 8416.
Supplemental material for this article may be found at http://dx.doi.org/10.1128/AAC.00169-13.

doi:10.1128/AAC.00169-13

(14). Compared to the native peptide, this TempL analog exhibited improved bactericidal activity against two *Pseudomonas aeruginosa* strains among the tested Gram-negative bacteria (14). However, to our knowledge, there is no report on the antiendotoxin properties of (Arg^3)TL. In the present study, we incorporated a lysine residue in place of a glutamine residue at position 3 of TempL (Q3K-TempL), which ultimately added an extra charge to the parent molecule, and investigated its subsequent effects on the structural, functional, and antiendotoxin properties of the peptide. Biochemical and biophysical studies revealed the basis of augmentation of the antiendotoxin properties of TempL as a result of the introduction of an additional lysine residue.

MATERIALS AND METHODS

Rink amide MBHA resin (loading capacity, 0.63 mmol/g) and all *N*-α-Fmoc (9-fluorenylmethoxy carbonyl)- and side chain-protected amino acids were from Novabiochem. Coupling reagents for peptide synthesis, such as 1-hydroxybenzotriazole, *N*,*N*′-diisopropylcarbodiimide (DIC), 1,1,3,3-tetramethyluronium tetrafluoroborate, and *N*,*N*-diisopropylethylamine, were from Sigma, while dichloromethane, *N*,*N*-dimethylformamide, and piperidine were of standard grades and were procured from reputable local companies. Acetonitrile (high-performance liquid chromatography [HPLC] grade) was procured from Merck, whereas trifluoroacetic acid (TFA) was purchased from Sigma. 6-Carboxytetramethylrhodamine (TAMRA) was purchased from Invitrogen (Molecular Probes, Eugene, OR). *Escherichia coli* 0111:B4 lipopolysaccharide (L3012), *E. coli* 0111:B4 fluorescein isothiocyanate (FITC)-LPS (F3665), 8-anilinonapthalene-1-sulfonic acid (ANS) (A1028), and polymyxin B (P0972) were procured from Sigma. The rest of the reagents were of analytical grade and were procured locally. Buffers were prepared in Milli-Q ultrapure water (USF-ELGA).

Animals. All animal procedures were performed in accordance with the protocols approved by the Institutional Animal Ethics Committee (79/10/MSB/IAEC) and National Laboratory Animal Center (Lucknow, India). Animals were properly anesthetized before experiments, and all treatments were performed to minimize the suffering of the animals. Our animal protocols adhere to the guidelines of the Committee for the Purpose of Control and Supervision of Experiments on Animals (CPCSEA), Government of India.

Cell culture. Rat bone marrow-derived macrophages were obtained by inducing differentiation in bone marrow cells isolated from the marrow of the femurs of healthy wistar rats aged approximately 3 to 4 weeks. The differentiation was induced by previously known methods using the supernatant of L929 murine fibroblasts (15, 16). The culture and processing of these differentiated cells were performed in Dulbecco modified Eagle medium (Sigma 5648-1L) containing 10% fetal bovine serum (EU-000-F; Sera Laboratories, West Sussex, United Kingdom) supplemented with GIBCO antibiotic antimycotic (Invitrogen 100× antibiotic-antimycotic; 15240).

Peptide synthesis, fluorescent labeling and purification. The stepwise solid-phase synthesis of all the peptides was performed on rink amide MBHA resin (0.15 mmol) using standard Fmoc chemistry as reported previously (17). Labeling at the N termini of peptides with fluorescent probes, cleavage of the labeled and unlabeled peptides from the resins, and their HPLC purification were achieved by standard procedures (18, 19). Experimental molecular masses of the peptides were detected by electrospray ionization-mass spectrometry (ESI-MS) analysis.

Structural-parameter computation. Hydrophobic parameters, such as the mean hydrophobicity, hydrophobic moment, and mean relative hydrophobic moments, of peptides were calculated on the Eisenberg scale of hydrophobicity. *In vitro* aggregation and secondary-structure prediction were performed by use of TANGO software (20). The peptide's net hydrophobic mean character was calculated by the GRAVY (grand average of hydropathy) scale (21).

Hemolytic activity of the peptides. Hemolytic activity of the peptides against human red blood cells (hRBCs) in phosphate-buffered saline (PBS) was examined to determine the cytotoxic activity of the peptides, as reported previously (19).

Assay for evaluation of LPS-neutralizing activity. Cultured rat bone marrow-derived macrophages at 5×10^5 cells/well in 24-well plates were stimulated with *E. coli* LPS O111:B4 (100 ng/ml) in the presence of 2.5, 5, or 10 μM TempL and its designed analog Q3K-TempL. Cells stimulated with LPS alone and untreated cells were used for maximum and minimum cytokine production in a given set of experiments. The cells were later incubated for 6 h at 37°C in an incubator. Afterward, samples of the medium from each treatment were collected. Concentrations of tumor necrosis factor alpha (TNF-α) and interleukin 6 (IL-6) in the samples were evaluated using mouse enzyme-linked immunosorbent assay kits for TNF-α (BD Biosciences catalog no. 558534) and IL-6 (BD Biosciences catalog no. 555240) according to the manufacturers' protocol, and data were presented in terms of percentage inhibition of LPS-induced cytokine production in the presence of these peptides.

Trypan blue cell exclusion assay. After LPS and peptide treatments, the viability of macrophages was tested by trypan blue cell exclusion assay as previously described (22–24). Following the LPS and peptide treatments, the cells were washed with chilled PBS (pH 7.4), and later, trypan blue (4-mg/ml) solution was added to the cells for 2 min. Trypan blue staining of cells from each treatment group was estimated by using a hemocytometer under an inverted microscope.

Tryptophan fluorescence experiments with LPS. Increasing concentrations of LPS were added to a solution of TempL or its designed analog (5 μM final concentration) in HEPES buffer (5 mM HEPES, 0.1 mM EDTA, pH 7.0), and fluorescence spectra were measured in a quartz cuvette with a Perkin-Elmer LS55B spectrometer with emission and excitation slits set at 8 and 6 nm. The tryptophan residue of Temporin L was excited at 280 nm, and emission spectra were recorded between 300 and 400 nm, with averaging of two scans. Spectra were recorded as a function of the lipid/peptide molar ratio and corrected for the contribution of light scattering in the presence of lipid vesicles. Blue shifts were measured as the differences in wavelength of the maxima in emission spectra of lipid-peptide and peptide samples.

CD spectroscopy. We performed circular-dichroism (CD) experiments to study the propensity of TempL and its analog to self-assemble in LPS and aqueous environments. For this purpose, dose-dependent CD spectra of the peptides were recorded in the presence of LPS and in PBS (pH 7.4; 1.5 M NaCl) (25) by employing a Jasco J-500A spectropolarimeter, which was calibrated with (+)-10-camphorsulfonic acid. Spectra of the samples were recorded at 30°C in a capped quartz optical cell with a path length of 0.2 cm in the wavelength range of 250 to 190 nm. Mean residue ellipticity values expressed in terms of [θ] (degrees square centimeters per decimole) were determined as reported previously (19, 26).

LPS destabilization induced by the peptides. Collapse of the diffusion potential of the LPS membrane due to disintegration of LPS core structure was detected fluorimetrically, as described previously (27). The LPS large unilamellar vesicle (LUV) suspension (10 mg/ml in 200 μl) prepared in K buffer (50 mM K_2SO_4 and 25 mM HEPES sulfate [pH 6.8]) was added to an isotonic K-free buffer (50 mM Na_2SO_4 and 25 mM HEPES sulfate [pH 6.8]) to a final concentration of 50 μg/ml LPS. Then, the membrane-sensitive probe di-S-C_{3-5}, followed by subsequent addition of valinomycin (0.1 μM), created a negative diffusion potential inside the vesicles. Peptide-induced membrane perturbation caused the membrane diffusion potential to dissipate, resulting in an increase in fluorescence. The fluorescence was monitored using excitation and emission wavelengths of 620 and 670 nm, with the bandwidth kept at 8 and 6 nm, respectively.

Detection of peptide-induced dissociation of LPS aggregates. To study the effects of treatments with TempL or Q3K-TempL on the physical state of LPS, we assayed the peptide-induced disaggregation of LPS by employing FITC-labeled LPS, as reported previously (25, 28). FITC-LPS

(0.5 μg/ml) was treated with increasing concentrations of either TempL or its analog from 10 μM to 100 μM. The changes in the emission of FITC-LPS as a function of change in the aggregation state of LPS in 10 mM sodium phosphate buffer (pH, 6.9) were monitored at 515 nm using a fluorescence spectrometer (Perkin-Elmer LS55) with the excitation wavelength set at 488 nm and excitation and emission slits at 8 and 6 nm, respectively. The fluorescence data for FITC-LPS at 515 nm were collected with or without peptide addition after background subtraction. Peptide-induced dissociation of the aggregated state of FITC-LPS was measured as an increase in its fluorescence (25, 29).

Binding of peptides to endotoxin (LAL assay). The abilities of TempL and its designed analog Q3K-TempL to bind LPS were assessed using a quantitative chromogenic *Limulus* amoebocyte lysate (LAL) with a QCL-1000 (Lonza 50-647U) kit. Experiments were carried out following the protocols recommended by the manufacturer. Stock solutions of peptides were prepared in pyrogen-free water provided with the kit. Peptides at concentrations of 1.875, 3.75, 7.5, and 15 μM were incubated with 0.5 endotoxin units (EU) of LPS in nonpyrogenic microtubes at 37°C for 30 min to allow the binding of peptides to LPS. A total of 50 μl of this mixture was then added to an equal volume of LAL reagent (50 μl), and the mixture was further incubated for 10 min, followed by the addition of 100 μl of LAL chromogenic substrate (Ac–Ile–Ala–Arg–*p*-nitroaniline). The reaction was terminated by the addition of 25% acetic acid, and the yellow color that developed due to cleavage of the substrate was measured spectrophotometrically at 410 nm. The reduction of absorbance at 410 nm as a function of the peptide concentration is directly proportional to the inhibition of LPS by the peptide (30, 31).

Oligomerization of TempL and Q3K-TempL associated with LPS by Tris-Tricine SDS gel electrophoresis. TempL and Q3K-TempL (~30 μg) were incubated with LPS at 37°C for 30 min. Peptide-LPS complexes were treated with freshly prepared solutions of bis-(sulfosuccinimidy1)-suberate (BS^3) (Pierce) at 37°C for 10 min. The reaction was quenched by addition of 1/3 volume of 10 mM MOPS (morpholinepropanesulfonic acid) buffer, pH 7.4, containing 50 mM NaCl and 50 mM lysine (32). Each reaction mixture was treated with polyacrylamide gel electrophoresis (PAGE) loading buffer containing 1% SDS and 5% 2-mercaptoethanol. The peptide-LPS conjugates were subjected to SDS-PAGE in 16.5% Tris-Tricine acrylamide gels, as reported previously (33). An equal amount of the peptides without addition of LPS was also processed similarly for gel electrophoresis experiments after treatment with BS^3 and loading buffer to investigate the relative state of peptide oligomerization in the absence of LPS. Images of Coomassie blue-stained gels were taken and analyzed with respect to the apparent molecular weight marker.

ANS fluorescence measurements. To investigate the relative change in the extent of oligomerization in TempL and Q3K-TempL with the addition of LPS in peptide solutions, we performed ANS binding assays with peptides preincubated with LPS. Aliquots of ANS (10 mM stock) were added to a peptide-lipid complex preincubated for 30 min at 37°C. Fluorescence intensities were measured at emission wavelengths ranging from 400 to 600 nm using an excitation wavelength of 365 nm in PBS at room temperature. For control experiments, the peptides at equal concentrations were treated with ANS to observe the relative difference in peak shift in the peptides' maxima when added to lipids. The background fluorescence of ANS in lipids and buffer were subtracted from the spectra obtained (34).

Fluorescence anisotropy experiment with FITC-LPS. Fluorescence anisotropy measurements of FITC-LPS (1 μg/ml) in the presence of TempL and Q3K-TempL were performed with a Perkin-Elmer spectrofluorimeter using 10 mM sodium phosphate buffer, pH 6.0. Excitation and emission wavelengths were set at 470 and 515 nm, and both bandwidths were set at 10 nm. For each sample, fluorescence emission intensity data in parallel and perpendicular orientations with respect to the exciting beam were collected 10 times each and then averaged. Anisotropy (r) was calculated as follows: $r = (I - GI_{\perp})/(I + 2GI_{\perp})$, where I and $I_{\perp}$ are the parallel and perpendicular polarized intensities measured with the vertically polarized excitation light and G is the monochromator grating correction factor (35). Final anisotropy values were determined after subtracting control anisotropy readings of increasing concentrations of each peptide from the corresponding FITC-LPS and peptide complex in the same solvent.

Detection of the aggregation state of TempL and Q3K-TempL by recording the proteolytic cleavage of their rhodamine-labeled analogs. An increase in rhodamine fluorescence following the treatment of proteinase K with a rhodamine-labeled peptide is implicated in the aggregated state of the peptide (36, 37). Thus, by looking at the relative enhancement in fluorescence of rhodamine-labeled TempL and its analog following the proteinase K treatment, it is possible to have a qualitative understanding of the aggregation states of these peptides in an aqueous environment. The changes in fluorescence of rhodamine-labeled TempL or Q3K-TempL (both at 0.25 μM) after the addition of proteinase K (100 μg/ml) was measured with respect to the time in PBS. The excitation and emission wavelengths were set at 550 and 570 nm, respectively, with excitation and emission slit widths at 8 and 6 nm, respectively.

***In vivo* studies of antiendotoxin properties of the peptides.** Female BALB/c mice were given a standard laboratory diet and water *ad libitum* and housed under controlled environmental conditions (National Laboratory Animal Center, Central Drug Research Institute, Lucknow, India). They were approximately 30 g each at the start of the experiments. All the mice were divided into experimental groups of 5 each for LPS, peptide, or LPS and peptide administration. To examine the efficacies of the peptides in neutralizing the LPS-induced inflammatory response in mice, the mice were first injected with 10 mg/kg of body weight *E. coli*-derived 0111:B4 LPS, followed (in ~5 to 7 min) by the addition of the respective peptide, TempL or its analog, at different sites of intraperitoneal (i.p.) administration. Similar to the peptide treatments, polymyxin B (1 mg/kg) was administered to LPS-treated mice to observe the inhibition of LPS-induced proinflammatory responses in mice and employed as a positive control. The mice treated with only saline or TempL (1 mg/kg) or Q3K-TempL (0.25 mg/kg) were considered experimental controls to monitor the basal proinflammatory-cytokine levels and peptide-induced proinflammatory responses in mice without LPS stimulation. The animals under different kinds of treatment, as mentioned above, were kept under observation for 72 h. The survival of the mice was monitored for 72 h after LPS and/or peptide administration. For serum TNF-α and IL-6 measurement, mice were anesthetized with ether, and blood was collected via either tail vein or orbital sinus aseptically. Serum TNF-α and IL-6 levels were determined with enzyme-linked immunosorbent assay kits, as mentioned above. Endotoxin concentrations were measured with the commercially available *Limulus* amoebocyte lysate test (QCL-1000-LONZA 50-647U) kit. Plasma samples were diluted with sterile endotoxin-free water. The endotoxin content was determined as described by the manufacturer, and the concentrations of endotoxin were calculated by comparison with the standard curve.

Calculation of the therapeutic index. The therapeutic indexes of TempL and its analog were calculated to analyze the efficiency of TempL and Q3K-TempL, as described previously (38). We estimated the therapeutic potentials of TempL and Q3K-TempL by calculating the ratio of the MHC_{50} (the minimum concentration of peptide that induces 50% hemolysis in hRBCs) and $MIC_{antiendotoxin}$ (the minimum peptide requirement [mg/kg] to attenuate the lethal cytokine response and maintain survival of LPS-treated mice) related to the antibacterial and antiendotoxin efficacies of the peptides, respectively.

Statistical analysis. Each experiment was repeated three times, and the results were expressed as means ± standard deviations. The data were analyzed statistically using Prism 3.0 software. Statistical analysis was performed using analysis of variance with the Newman-Keuls test. A P value of <0.05 was considered statistically significant, whereas a P value of >0.5 was insignificant.

A

Peptide	Sequence	Cal.mass	Observed Mass	RP-HPLC Retention time
TempL	X-NH- F V Q W F S K F L G R I L-CONH$_2$	1641.12	1641	~21.0 min
Q3K,TempL	X-NH- F V K W F S K F L G R I L-CONH$_2$	1641.16	1642	~19.0 min

B

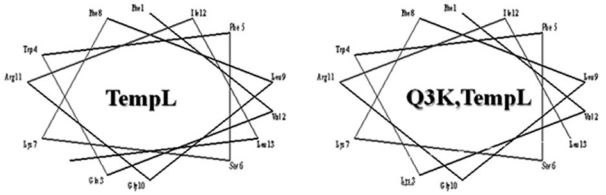

FIG 1 Sequences, molecular masses, helical-wheel projections, and physical properties of TempL and its analog. (A) Amino acid sequences of the peptides, their calculated (Cal.) and ESI-MS observed molecular masses, and reverse-phase (RP)-HPLC retention times for TempL and Q3K-TempL in a water-acetonitrile gradient system (80% to 20% in 40 min at a 0.7-ml/min flow rate). (B) Helical-wheel projections of TempL and Q3K-TempL.

RESULTS AND DISCUSSION

Design and synthesis of a novel analog of Temporin L. The overall biological activity of TempL is governed greatly by the hydrophobic and minimally by the hydrophilic characters of the peptide. Moreover, the number of cationic residues in TempL is only two, which is less than in other antimicrobial peptides of similar lengths (39, 40). A closer examination of the sequence of TempL revealed that there is scope to increase the balance between cationic and hydrophobic residues. Further, as mentioned in the introduction, by employing related algorithms we found that a replacement of glutamine with lysine at the third position of TempL could significantly reduce its aggregation propensity in an aqueous environment. Therefore, we chose to replace the glutamine residue at this position in TempL with a lysine residue. Further, lysine possesses a molecular mass, polar character, and helical propensity very similar to those of glutamine. The amino acid sequences, HPLC retention times, and helical wheels are shown in Fig. 1.

Structural-parameter computation. To characterize the physicochemical properties of Q3K-TempL and the parent peptide, TempL, several structural parameters were calculated (Table 1) by using available methodologies. The higher values of μ and μ-rel (calculated on the basis of the Eisenberg scale) for Q3K-TempL (Table 1) than for TempL (0.44 and 0.54 versus 0.41 and 0.51) indicate its greater tendency to form helices than the parent peptide, which was verified by their relative helicities in 30% trifluoroethanol (data not shown). The reduced mean hydrophobicity of Q3K-TempL (0.03) compared to TempL (0.06) implies its enhanced polar character compared to the parent peptide. The aliphatic index and GRAVY indicated equivalent amphipathies (112.31 [Table 1]) for the two peptides and lesser hydrophobic character for Q3K-TempL (0.792) than TempL (0.823). Amylo values calculated by TANGO (20, 21) showed significantly lower values for Q3K-TempL (2,796.92) than for TempL (,4794.7) and indicated less *in vitro* aggregation behavior of the TempL analog than its parent peptide (Table 1).

TABLE 1 Physicochemical parameters[a] of TempL and the designed analog

Peptide	<H>	μ	μ-rel	Aliphatic index	GRAVY	Amylo
TempL	0.06	0.41	0.51	112.31	0.823	4,794.7
Q3K-TempL	0.03	0.44	0.54	112.31	0.792	2,796.92

[a] <H>, mean hydrophobicity; μ, hydrophobic moment; μ-rel, mean relative hydrophobic moment; amylo, amylogenic properties of peptides.

The designed analog of TempL exhibited significantly higher *in vitro* LPS neutralization ability than the parent peptide. TempL is known to inhibit LPS-induced proinflammatory responses in macrophages *in vitro* by up to 50 to 60% at nontoxic concentrations (41). We studied TNF-α and IL-6, the two key cytokines associated with LPS-stimulated proinflammatory responses in rat macrophages, and observed that the levels of these cytokines in cell culture supernatant media were 2 to 3 times lower in the presence of Q3K-TempL than in the presence of TempL at all tested peptide concentrations ($P < 0.001$) (Fig. 2A and B). The viability of the macrophages after the experiment was checked by a trypan blue cell exclusion assay (Fig. 2C), which ruled out any significant cytotoxicity of the peptides for the macrophages ($P > 0.05$).

Marginal difference between TempL and its analog in their cytotoxic activities. To determine the cytotoxic activities of the peptides, the hemolytic activities of Temporin L and Q3K-TempL against hRBCs were measured. With a gradual increase in peptide concentrations, TempL and its analog showed progressively increasing hemolytic activity against hRBCs. Q3K-TempL exhibited marginally higher hemolytic activity (Fig. 3) than TempL ($P < 0.001$). Thus, the results indicate that the replacement of glutamine by lysine to some extent enhances the cytotoxicity of TempL. The data add to the literature on the studies with replacement of an amino acid(s) with a lysine residue(s) in a similar-size peptide, indolicidin (42, 43), and together suggest that the overall amino acid sequence of the parent peptide and the nature and position of the amino acid(s) that is replaced by a lysine residue(s) probably determine the effects of such amino acid substitutions.

TempL and Q3K-TempL showed differences in tryptophan fluorescence in LPS vesicles. Both peptides showed significant blue shifts of tryptophan emission maxima in the presence of increasing concentrations of LPS vesicles. However, a significant difference between the tryptophan emission maxima of TempL and Q3K-TempL in the presence of LPS vesicles was observed (see Fig. S1A in the supplemental material). For example, at 10- and 20-μg/ml LPS concentrations, TempL exhibited emission maxima of 356 nm and 350 nm, whereas under the same conditions,

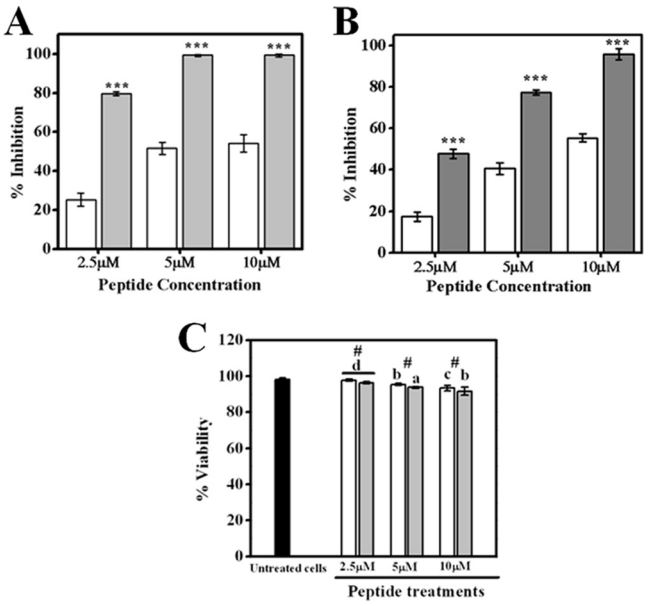

FIG 2 Effects of treatment with TempL and Q3K-TempL on production of proinflammatory cytokines by rat bone marrow-derived macrophages stimulated with LPS (100 ng/ml). (A) Percent inhibition of LPS-induced TNF-α production in macrophages by TempL (open bars) and Q3K-TempL (shaded bars) at concentrations of 2.5 μM, 5 μM, and 10 μM, as marked. (B) Percent inhibition of LPS-induced IL-6 production in macrophages by TempL (open bars) and Q3K-TempL (shaded bars) at concentrations of 2.5 μM, 5 μM, and 10 μM. (C) Data on percent viability of macrophages after the above-described experiments at different peptide concentrations, namely, 2.5 μM, 5 μM, and 10 μM, as indicated. In order to calculate the percentages of inhibition of cytokine production in LPS-stimulated macrophages by TempL and its analog, the amounts of cytokines produced in non-LPS-treated and LPS-treated cells (without addition of peptides) were taken as control values for minimum and maximum cytokine production levels for a given experimental set. (A and B) Results are presented as means ± standard deviations (SD); $n = 3$. ***, $P < 0.001$ versus TempL. (C) Results are presented as means ± SD; $n = 3$; #, $P > 0.05$ with respect to TempL; $P < 0.001$ (a), $P < 0.01$ (b), $P < 0.05$ (c), and $P = 0.005$ (d) versus untreated cells.

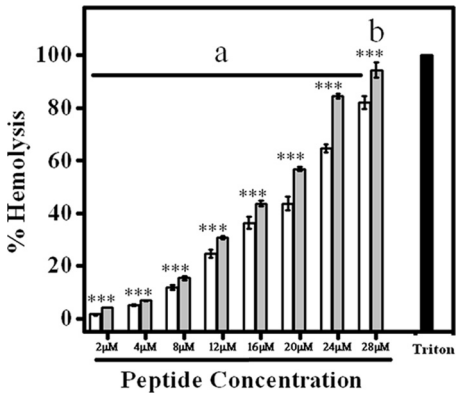

FIG 3 Dose-dependent hemolytic activities of TempL and Q3K-TempL against 6% hRBCs. Open bars, TempL; shaded bars, Q3K-TempL. The results are presented as means ± SD; $n = 3$. ***, $P < 0.001$ versus TempL; $P < 0.001$ (a) and $P < 0.01$ (b) versus absolute hemolysis (Triton-treated hRBCs).

Q3K-TempL showed emission maxima at 347 nm and 341.5 nm, respectively. This higher blue shift of the emission maximum of Q3K-TempL in LPS probably indicates that the tryptophan residue of Q3K-TempL is located toward the more hydrophobic environment of LPS compared to that of its native peptide. The results further suggest that the replacement of the glutamine residue by a lysine residue in TempL probably altered its mode of binding and/or conformation in LPS.

Fluorescence anisotropy experiment with FITC-LPS. The binding of TempL and its analog to LPS in solution was followed by recording the changes in fluorescence anisotropy of FITC-LPS in the presence of the peptides (see Fig. S2B in the supplemental material). The formation of FITC-LPS–peptide complexes led to a significant increase in fluorescence anisotropy, indicating that the binding of TempL or Q3K-TempL to LPS caused mechanical restrictions to the rotational mobility of FITC-LPS. However, the greater increase in anisotropy of FITC-LPS when it was bound to Q3K-TempL could be attributed to its stronger binding to the TempL analog than to TempL, resulting in its more restricted movement.

Q3K-TempL exhibited greater self-assembly in the LPS environment than TempL. The ellipticity values for both peptides increased in a dose-dependent manner in the LPS environment, but Q3K-TempL exhibited appreciably higher ellipticity values than TempL (Fig. 4A). The data indicate that Q3K-TempL possesses a greater tendency to self-assemble in LPS than its parent peptide. In this experiment, we noticed that at a higher peptide concentration the ellipticity values for both peptides were reduced, which indicates that at certain concentrations, both TempL and Q3K-TempL probably undergo a process to form insoluble aggregates, and this tendency was more prominent for TempL than Q3K-TempL.

Q3K-TempL exhibited greater self-assembly in the presence of LPS than TempL. The fluorescence yield of ANS increases significantly upon its transfer from the aqueous environment to a hydrophobic environment, and its emission maximum shifts toward a shorter wavelength (44). Since self-association of a peptide often involves the rearrangement of its hydrophobic residues, which creates well-defined hydrophobic patches, ANS is a suitable probe to detect the aggregation property of a peptide. We observed that in the presence of LPS, Q3K-TempL induced a marked increase in the fluorescence intensity of ANS concomitant with the blue shift of its emission maximum (Fig. 4B). However, in the same experiment, TempL did not induce any significant enhancement of ANS fluorescence or blue shift of its emission maximum. The results indicate that Q3K-TempL possesses better self-association properties in LPS than its parent peptide.

Q3K-TempL forms higher oligomeric states in the presence of LPS than TempL. The oligomeric states of the peptides in the presence and absence of LPS were investigated by using BS^3 cross-linker with the help of SDS-polyacrylamide gel electrophoresis experiments. The experiments revealed that Q3K-TempL formed higher oligomeric states ranging from dimers to octamers in LPS (Fig. 4C), whereas TempL oligomers were mostly limited to dimeric forms. In control experiments, TempL and Q3K-TempL were treated with BS^3 without prior incubation with LPS to investigate the intrinsic oligomeric states of the peptides in the aqueous phase stabilized by the cross-linker. We observed lower oligomeric states for both peptides in the aqueous environment than in the presence of LPS. The data indicate that in the presence of LPS, TempL and Q3K-TempL both undergo self-assembly/oligomerization, although Q3K-TempL exhibits a higher oligomeric state.

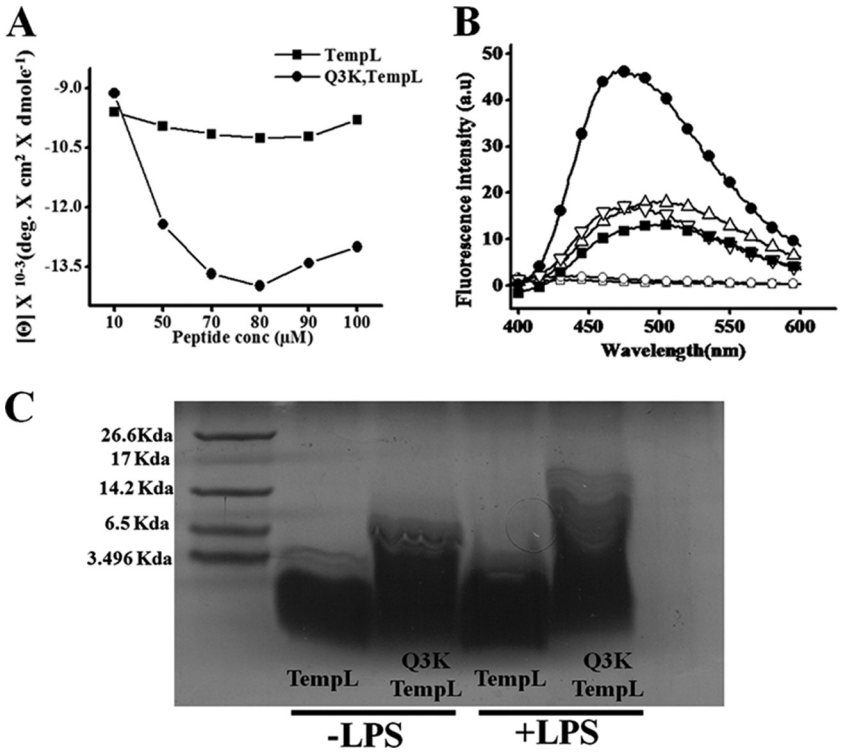

FIG 4 Determination of oligomerization/self-aggregation of TempL and Q3K-TempL in an LPS environment. (A) Molar ellipticity values for TempL and Q3K-TempL in an LPS (12.5 μM) environment; peptide concentrations were progressively increased, keeping the LPS concentration (12.5 μM) constant in phosphate-buffered saline. (B) Emission spectra of ANS (50 μM) in the presence of TempL and Q3K-TempL. □ and ○, emission spectra of TempL and Q3K-TempL, respectively, without ANS treatment; △ and ▽, ANS emission spectra in the presence of TempL and Q3K-TempL, respectively, in an aqueous environment; ■ and ●, ANS emission spectra in the presence of TempL and Q3K-TempL, respectively, in an LPS environment (50 μg/ml). The concentration of either TempL or Q3K-TempL was 10 μM in all experiments. (C) States of oligomerization of TempL and Q3K-TempL in the absence and presence of LPS as observed in a Tris-Tricine gel experiment. From left, lane 1, molecular mass markers; lanes 2 and 3, self-oligomeric states of TempL (30 μg) and Q3K-TempL (30 μg), respectively, stabilized with BS^3 in an aqueous environment (PBS); lanes 4 and 5, oligomeric states of TempL and Q3K-TempL (30 μg), respectively, in the presence of LPS (10 μg), stabilized by BS^3 treatment.

Q3K-TempL induced greater permeabilization in LPS vesicles than TempL. We examined whether TempL and its analog can disintegrate the core structure of the LPS membrane. For this purpose, dissipation of the diffusion potential across the LPS bilayer membrane in the presence of TempL and Q3K-TempL was measured (Fig. 5A and B). Q3K-TempL showed significantly higher permeabilization in LPS vesicles than TempL. Further, the results may be implicated in the greater ability of Q3K-TempL to destabilize the organization of the bilayered structure of LPS vesicles.

Q3K-TempL dissociates LPS aggregates with greater efficacy than TempL. The physical state of LPS seems to play a key role in determining the LPS-stimulated proinflammatory responses, and a direct relationship has been found between most of the LPS-neutralizing peptides and their respective abilities to dissociate the aggregated state of LPS (45–48). Q3K-TempL induced the dequenching of FITC-LPS fluorescence more prominently than TempL (Fig. 5C), which suggests that the designed TempL analog can induce greater disintegration of LPS oligomers than the native peptide. However, TempL-induced dissociation to some extent can be correlated with its lesser LPS-neutralizing ability.

Q3K-TempL possesses greater LPS neutralization ability than TempL. The effect of introduction of a lysine residue to the N terminus of TempL on its binding to LPS was examined by performing the chromogenic LAL assay with TempL and Q3K-TempL by employing an endotoxin detection kit (Fig. 6). Binding of the peptides to LPS was determined by measuring their efficacy to inhibit the LPS-induced activation of the LAL enzyme. TempL and its designed analog, Q3K-TempL, showed significant binding to LPS, as evidenced by the substantial inhibition of activation of the LAL enzyme ($P < 0.001$). However, Q3K-TempL showed considerably greater inhibition of the LAL enzyme than TempL at all concentrations employed ($P < 0.001$); for example, at 7.5 μM, TempL showed only 17% inhibition of the LAL enzyme while Q3K-TempL exhibited 92% inhibition of the LAL enzyme as a consequence of higher LPS binding efficiency (Fig. 6).

Q3K-TempL inhibited proinflammatory mediators in a more pronounced manner and promoted the survival of LPS-treated BALB/c mice at a lower concentration than TempL. The inhibitory effects of TempL on LPS-stimulated production of TNF-α and IL-6 in macrophages have been examined (41), and the implication of these two cytokines in endotoxemia is well documented (49, 50). Therefore, we chose the two cytokines as markers of LPS-induced proinflammatory response either in macrophages or in BALB/c mice. A significant decline in production of the proinflammatory cytokines TNF-α and IL-6 in LPS-stimulated primary rat macrophages in the presence of TempL and its analog was observed (Fig. 2). Further, we investigated the changes

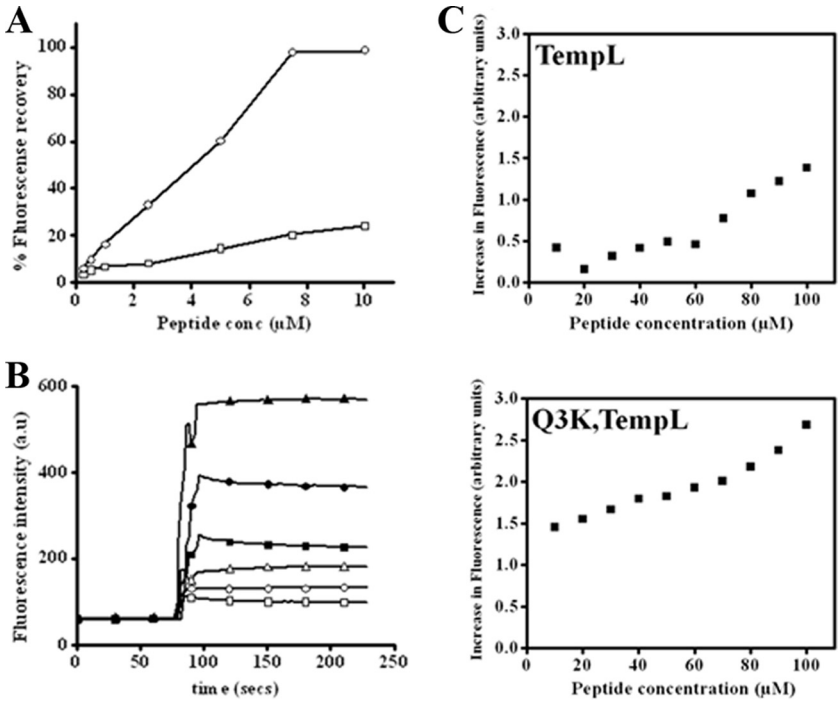

FIG 5 (A) Dissipation of the diffusion potential of LPS vesicles in the presence of TempL and its analog. The plot shows the percentage fluorescence recovery induced by increasing concentrations of TempL (□) and Q3K-TempL (○). (B) Representative fluorescence profiles for dissipation of diffusion potential induced by TempL and Q3K-TempL in LPS vesicles. The open symbols represent TempL, and the closed symbols represent Q3K-TempL. Shown are peptide concentrations of 2.5 μM (squares), 5 μM (circles), and 10 μM (triangles). (C) Increase in fluorescence (arbitrary units) of FITC-LPS as a result of peptide-induced dissociation of its aggregates plotted with respect to the concentrations of the peptides. FITC-LPS (0.5 μg/ml) was treated with various concentrations of peptides to detect the dissociation of LPS aggregates as evidenced by dequenching of its fluorescence. The collected fluorescence data with a particular peptide (TempL or Q3K-TempL) are shown on the *y* axis of each plot.

in serum levels of these proinflammatory cytokines over time after LPS administration (10 mg/kg i.p.) in BALB/c mice. As shown in Fig. 7A and B, serum TNF-α and IL-6 levels, which were negligible in the untreated-mouse group, rose significantly at higher levels after administration of LPS ($P < 0.001$). The group of LPS (10-mg/kg)-treated mice when further treated with TempL (1 mg/kg) or Q3K-TempL (0.25 mg/kg) demonstrated appreciable inhibition of the cytokine levels in serum ($P < 0.001$), as with polymyxin B treatment of mice, administered LPS ($P < 0.001$), which served as a positive control for inhibitory activity against the LPS-induced proinflammatory responses (Fig. 7A and B). However, when the mice administered LPS were treated with TempL at a lower dose (0.25 mg/kg), only partial inhibition of the LPS-induced proinflammatory response was observed, as evidenced by the serum IL-6 and TNF-α levels. Detailed statistical analyses of the same data are provided in Fig. S3 in the supplemental material.

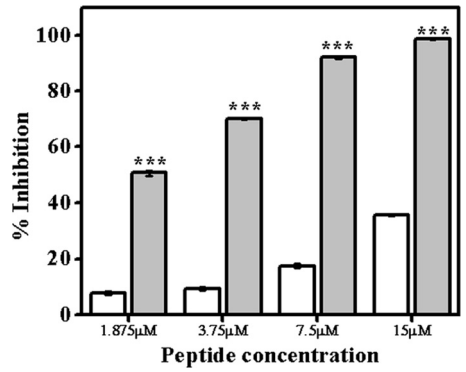

FIG 6 Binding of TempL and Q3K-TempL to LPS was determined by quantitative chromogenic LAL assay. The efficiencies of TempL and Q3K-TempL in binding to LPS were analyzed by estimating their abilities to inhibit the LPS-mediated activation of LAL enzyme. Inhibition of substrate color production as a function of inhibition of LAL enzyme activity was estimated, and the percentage LPS binding was calculated. Binding of TempL (open bars) and Q3K-TempL (shaded bars) to LPS is denoted by the percentage of inhibition of color production at various peptide concentrations, namely, 1.875, 3.75, 7.5, and 15.0 μM. The results are presented as means ± SD; $n = 3$. ***, $P < 0.001$ versus TempL.

Further, LPS-treated mice showed nearly 10-fold-higher endotoxin levels in blood serum, which was successfully attenuated by Q3K-TempL (0.25 mg/kg) and TempL (1 mg/kg) ($P < 0.001$). Though TempL (0.25 mg/kg) inhibited such a rise in endotoxin levels in mouse blood, it was not comparable to the attenuation obtained with Q3K-TempL at a similar concentration (Fig. 7C) ($P < 0.001$). This result also verifies that Q3K-TempL is more potent than its parent peptide in neutralizing LPS-induced proinflammatory response *in vivo* in mice. Our control experimental mouse groups, such as mice administered LPS and subsequently treated with polymyxin B (marked as "P" for polymyxin B) or mice treated with either TempL or Q3K-TempL alone, exhibited minimal levels of blood serum endotoxin, denoting maximum inhibition of LPS by polymyxin B and the nonpyrogenic nature of TempL or Q3K-TempL, respectively (Fig. 7C).

We obtained significant mortality in LPS-treated mice compared to the untreated group of mice ($P < 0.001$). However, the

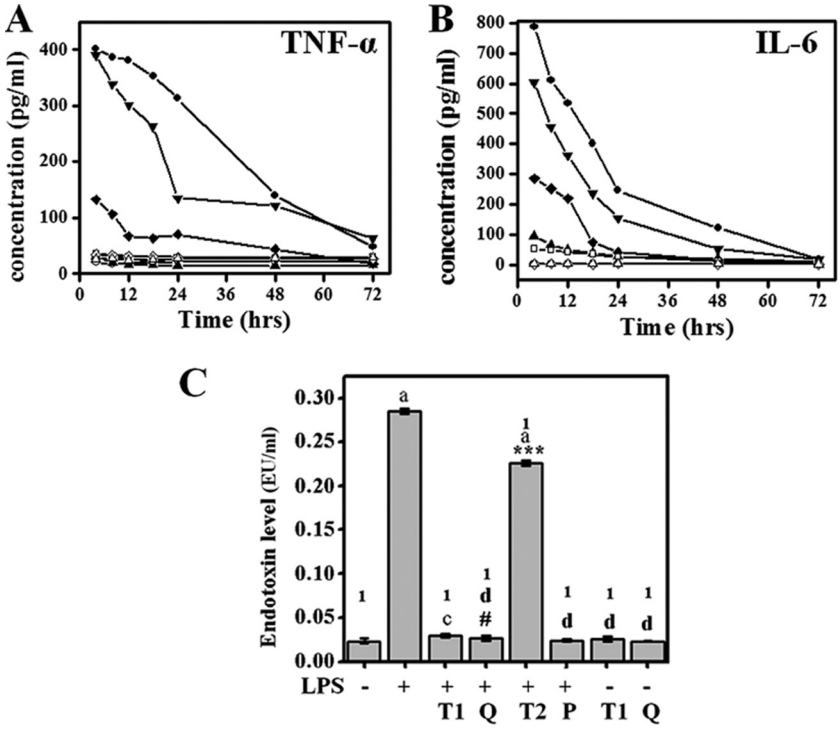

FIG 7 Alterations in the levels of proinflammatory cytokines with time in the sera of LPS-treated (LPS 0111:B4; 10 mg/kg) BALB/c mice in the absence and presence of TempL and Q3K-TempL (as described in Materials and Methods). (A) TNF-α levels in blood sera of LPS- and peptide-treated mice at different time intervals. (B) IL-6 concentrations in blood sera of LPS- and peptide-treated mice at different time intervals. Squares, mice not treated with peptide or LPS; circles, mice treated with LPS only (10 mg/kg); triangles, mice treated with TempL (1 mg/kg) and LPS; inverted triangles, mice treated with Q3K-TempL (0.25 mg/kg) and LPS; diamonds, mice treated with TempL (0.25 mg/kg) and LPS; left arrowheads, mice treated with polymyxin B (1 mg/kg) and LPS; right arrowheads, mice treated with TempL (1 mg/kg) with no LPS; hexagons, mice treated with Q3K-TempL (0.25 mg/kg) with no LPS. (C) Endotoxin concentrations in blood sera of LPS- and peptide-treated mice after 6 h of peptide or LPS administration. The results are presented as means ± SD; $n = 3$. ***, $P < 0.001$, and #, $P > 0.05$ versus TempL. $P < 0.001$ (a), $P < 0.01$ (b), $P < 0.05$ (c), and $P = 0.0.05$ (d) versus untreated mice and $P < 0.001$ (1) versus LPS-treated mice. + and −, treatment or no treatment with LPS. Peptide treatments: T1, TempL (1 mg/kg); Q, Q3K-TempL (0.25 mg/kg); T2, TempL (0.25 mg/kg); P, polymyxin B (1 mg/kg).

mouse groups first treated with LPS and then administered either TempL (1 mg/kg) or Q3K-TempL (0.25 mg/kg) showed resistance to the lethal effects of LPS ($P < 0.001$). The higher LPS neutralization by Q3K-TempL was also evident from the absolute survival of LPS-treated mice when administered Q3K-TempL (0.25 mg/kg) compared to the LPS-treated mice administered the same dose of TempL (0.25 mg/kg) (see Table S1 in the supplemental material), which failed to survive LPS toxicity. Polymyxin B showed prominent attenuation of LPS toxicity in mice and absolute survival (survival of all the experimental animals) of LPS-treated mice ($P < 0.001$). The control group of mice, treated with TempL or Q3K-TempL only in the absence of LPS, also showed no sign of inflammatory stress and both peptides did not induce mortality in treated mice ($P < 0.001$ compared to LPS-treated mice) (see Table S1 in the supplemental material). Probably, the data further indicate that at the levels used the peptides *per se* were not toxic to the mice.

The therapeutic potential of the peptides was determined with respect to their *in vivo* anti-LPS activity (see Table S1 in the supplemental material) in mice. It is evident that introduction of the lysine residue in place of the glutamine residue at the third position appreciably enhances the therapeutic potential of Temporin L with respect to the neutralization of the LPS-induced inflammatory response in mice (see Table S2 in the supplemental material).

The lysine residue introduced at the N terminus of TempL probably reduced the propensity and the extent of amyloid-like fibril formation by TempL in aqueous solution, as also predicted on the basis of amylo value in Table 1. In our preliminary experiments, thioflavin T showed appreciably strong fluorescence with TempL, while it showed significantly weak fluorescence in the presence of Q3K-TempL (unpublished results). Introduction of the lysine residue significantly reduced the aggregation state of TempL in an aqueous environment, as evidenced by recording the fluorescence of Rho-labeled peptides after proteolytic cleavage (see Fig. S2 in the supplemental material). To investigate the effect of the glutamine-to-lysine substitution on the bactericidal properties of TempL, antibacterial assays with the peptides were performed against two Gram-negative bacteria, namely, *E. coli* (ATCC 10536) and *P. aeruginosa* (ATCC BAA-427) (see Table S3 in the supplemental material). We observed nearly 2-fold increments in the bactericidal activity of Q3K-TempL against these Gram-negative bacteria in comparison to TempL, indicating that the replacement of glutamine by lysine at position 3 appreciably enhanced the bactericidal activity of Temporin L (see Table S3 in the supplemental material). The TempL analog with substitution of arginine at the same position also showed improved bactericidal activity against two *P. aeruginosa* strains among the tested Gram-negative bacteria (14).

In conclusion, in the course of investigating the structure-function relationship of a naturally occurring antimicrobial pep-

tide, TempL, we observed a correlation between the antiendotoxin properties (Fig. 2 and 7) of TempL and its aggregation in LPS (Fig. 4). The present study demonstrates how the introduction of a lysine residue toward the N terminus of aggregation-prone TempL can reduce its inherent propensity to aggregate in an aqueous environment and augment its oligomerization in LPS. The enhanced oligomeric state of Q3K-TempL probably led to its better binding to LPS and disintegration of LPS aggregates, resulting in the augmented neutralization of an LPS-induced proinflammatory response in rat macrophages *in vitro* and in mice *in vivo* by the peptide. The results presented here could be useful in developing potential anti-infective peptides.

ACKNOWLEDGMENTS

The work was supported by the Council of Scientific and Industrial Research (CSIR) network projects NWP 0005 and BioDiscovery. S.S. acknowledges the receipt of senior research fellowships from the CSIR, India.

Anshika Tandon is acknowledged for assisting in *in vivo* experiments with BALB/c mice. We are extremely grateful to A. L. Vishwakarma for recoding the flow cytometry profiles and Sanjeev Kanojiya, Sophisticated Analytical Instrumentation Facility (SAIF), CSIR-CDRI, for recording the ESI-MS mass spectra. We are very grateful to the anonymous reviewers for their valuable comments on improving the quality of the manuscript.

REFERENCES

1. **Hurley JC.** 1995. Endotoxemia: methods of detection and clinical correlates. Clin. Microbiol. Rev. **8**:268–292.
2. **Annane D, Bellissant E, Cavaillon JM.** 2005. Septic shock. Lancet **365**: 63–78.
3. **Luderitz O, Galanos C, Lehmann V, Nurminen M, Rietschel ET, Rosenfelder G, Simon M, Westphal O.** 1973. Lipid A: chemical structure and biological activity. J. Infect. Dis. **128**(Suppl.):17–29.
4. **Boman HG.** 1995. Peptide antibiotics and their role in innate immunity. Annu. Rev. Immunol. **13**:61–92.
5. **Lorenzon EN, Cespedes GF, Vicente EF, Nogueira LG, Bauab TM, Castro MS, Cilli EM.** 2012. Effects of dimerization on the structure and biological activity of antimicrobial peptide Ctx-Ha. Antimicrob. Agents Chemother. **56**:3004–3010.
6. **Knappe D, Fritsche S, Alber G, Kohler G, Hoffmann R, Muller U.** 2012. Oncocin derivative Onc72 is highly active against Escherichia coli in a systemic septicaemia infection mouse model. J. Antimicrob. Chemother. **67**:2445–2451.
7. **Bowdish DM, Davidson DJ, Scott MG, Hancock RE.** 2005. Immunomodulatory activities of small host defense peptides. Antimicrob. Agents Chemother. **49**:1727–1732.
8. **Majerle A, Kidric J, Jerala R.** 2003. Enhancement of antibacterial and lipopolysaccharide binding activities of a human lactoferrin peptide fragment by the addition of acyl chain. J. Antimicrob. Chemother. **51**:1159–1165.
9. **Andra J, Koch MH, Bartels R, Brandenburg K.** 2004. Biophysical characterization of endotoxin inactivation by NK-2, an antimicrobial peptide derived from mammalian NK-lysin. Antimicrob. Agents Chemother. **48**: 1593–1599.
10. **Piers KL, Brown MH, Hancock RE.** 1994. Improvement of outer membrane-permeabilizing and lipopolysaccharide-binding activities of an antimicrobial cationic peptide by C-terminal modification. Antimicrob. Agents Chemother. **38**:2311–2316.
11. **Vaara M, Nurminen M.** 1999. Outer membrane permeability barrier in Escherichia coli mutants that are defective in the late acyltransferases of lipid A biosynthesis. Antimicrob. Agents Chemother. **43**:1459–1462.
12. **Snyder DS, McIntosh TJ.** 2000. The lipopolysaccharide barrier: correlation of antibiotic susceptibility with antibiotic permeability and fluorescent probe binding kinetics. Biochemistry **39**:11777–11787.
13. **Mahalka AK, Kinnunen PK.** 2009. Binding of amphipathic alpha-helical antimicrobial peptides to lipid membranes: lessons from temporins B and L. Biochim. Biophys. Acta **1788**:1600–1609.
14. **Mangoni ML, Carotenuto A, Auriemma L, Saviello MR, Campiglia P, Gomez-Monterrey I, Malfi S, Marcellini L, Barra D, Novellino E, Grieco P.** 2011. Structure-activity relationship, conformational and biological studies of temporin L analogues. J. Med. Chem. **54**:1298–1307.
15. **Boltz-Nitulescu G, Wiltschke C, Holzinger C, Fellinger A, Scheiner O, Gessl A, Forster O.** 1987. Differentiation of rat bone marrow cells into macrophages under the influence of mouse L929 cell supernatant. J. Leukoc. Biol. **41**:83–91.
16. **Comalada M, Xaus J, Valledor AF, Lopez-Lopez C, Pennington DJ, Celada A.** 2003. PKC epsilon is involved in JNK activation that mediates LPS-induced TNF-alpha, which induces apoptosis in macrophages. Am. J. Physiol. Cell Physiol. **285**:C1235–C1245.
17. **Fields GB, Noble RL.** 1990. Solid phase peptide synthesis utilizing 9-fluorenylmethoxycarbonyl amino acids. Int. J. Pept. Protein Res. **35**:161–214.
18. **Verma R, Malik C, Azmi S, Srivastava S, Ghosh S, Ghosh JK.** 2011. A synthetic S6 segment derived from KvAP channel self-assembles, permeabilizes lipid vesicles, and exhibits ion channel activity in bilayer lipid membrane. J. Biol. Chem. **286**:24828–24841.
19. **Pandey BK, Srivastava S, Singh M, Ghosh JK.** 2011. Inducing toxicity by introducing a leucine-zipper-like motif in frog antimicrobial peptide, magainin 2. Biochem. J. **436**:609–620.
20. **Fernandez-Escamilla AM, Rousseau F, Schymkowitz J, Serrano L.** 2004. Prediction of sequence-dependent and mutational effects on the aggregation of peptides and proteins. Nat. Biotechnol. **22**:1302–1306.
21. **Torrent M, Andreu D, Nogues VM, Boix E.** 2011. Connecting peptide physicochemical and antimicrobial properties by a rational prediction model. PLoS One **6**:e16968. doi:10.1371/journal.pone.0016968.
22. **Kwok AK, Yeung CK, Lai TY, Chan KP, Pang CP.** 2004. Effects of trypan blue on cell viability and gene expression in human retinal pigment epithelial cells. Br. J. Ophthalmol. **88**:1590–1594.
23. **Kellum JA, Song M, Li J.** 2004. Lactic and hydrochloric acids induce different patterns of inflammatory response in LPS-stimulated RAW 264.7 cells. Am. J. Physiol. Regul. Integr. Comp. Physiol. **286**:R686–R692.
24. **Prabhakar SS, Zeballos GA, Montoya-Zavala M, Leonard C.** 1997. Urea inhibits inducible nitric oxide synthase in macrophage cell line. Am. J. Physiol. **273**:C1882–C1888.
25. **Srivastava RM, Srivastava S, Singh M, Bajpai VK, Ghosh JK.** 2012. Consequences of alteration in leucine zipper sequence of melittin in its neutralization of lipopolysaccharide-induced proinflammatory response in macrophage cells and interaction with lipopolysaccharide. J. Biol. Chem. **287**:1980–1995.
26. **Wu CS, Ikeda K, Yang JT.** 1981. Ordered conformation of polypeptides and proteins in acidic dodecyl sulfate solution. Biochemistry **20**:566–570.
27. **Papo N, Shai Y.** 2005. A molecular mechanism for lipopolysaccharide protection of Gram-negative bacteria from antimicrobial peptides. J. Biol. Chem. **280**:10378–10387.
28. **Bhunia A, Mohanram H, Bhattacharjya S.** 2009. Lipopolysaccharide bound structures of the active fragments of fowlicidin-1, a cathelicidin family of antimicrobial and antiendotoxic peptide from chicken, determined by transferred nuclear Overhauser effect spectroscopy. Biopolymers **92**:9–22.
29. **de Haas CJ, van Leeuwen HJ, Verhoef J, van Kessel KP, van Strijp JA.** 2000. Analysis of lipopolysaccharide (LPS)-binding characteristics of serum components using gel filtration of FITC-labeled LPS. J. Immunol. Methods **242**:79–89.
30. **Bhunia A, Mohanram H, Domadia PN, Torres J, Bhattacharjya S.** 2009. Designed beta-boomerang antiendotoxic and antimicrobial peptides: structures and activities in lipopolysaccharide. J. Biol. Chem. **284**:21991–22004.
31. **Schulke S, Waibler Z, Mende MS, Zoccatelli G, Vieths S, Toda M, Scheurer S.** 2010. Fusion protein of TLR5-ligand and allergen potentiates activation and IL-10 secretion in murine myeloid DC. Mol. Immunol. **48**:341–350.
32. **Onaderra M, Mancheno JM, Lacadena J, de los Rios V, Martinez del Pozo A, Gavilanes JG.** 1998. Oligomerization of the cytotoxin alpha-sarcin associated with phospholipid membranes. Mol. Membr. Biol. **15**: 141–144.
33. **Ahmad A, Azmi S, Ghosh JK.** 2011. Studies on the assembly of a leucine zipper antibacterial peptide and its analogs onto mammalian cells and bacteria. Amino Acids **40**:749–759.
34. **Kuo HH, Chan C, Burrows LL, Deber CM.** 2007. Hydrophobic interactions in complexes of antimicrobial peptides with bacterial polysaccharides. Chem. Biol. Drug Des. **69**:405–412.
35. **Garcia-Verdugo I, Sanchez-Barbero F, Soldau K, Tobias PS, Casals C.**

2005. Interaction of SP-A (surfactant protein A) with bacterial rough lipopolysaccharide (Re-LPS), and effects of SP-A on the binding of Re-LPS to CD14 and LPS-binding protein. Biochem. J. **391**:115–124.
36. **Rosenfeld Y, Barra D, Simmaco M, Shai Y, Mangoni ML.** 2006. A synergism between temporins toward Gram-negative bacteria overcomes resistance imposed by the lipopolysaccharide protective layer. J. Biol. Chem. **281**:28565–28574.
37. **Papo N, Oren Z, Pag U, Sahl HG, Shai Y.** 2002. The consequence of sequence alteration of an amphipathic alpha-helical antimicrobial peptide and its diastereomers. J. Biol. Chem. **277**:33913–33921.
38. **Jiang Z, Vasil AI, Gera L, Vasil ML, Hodges RS.** 2011. Rational design of alpha-helical antimicrobial peptides to target Gram-negative pathogens, Acinetobacter baumannii and Pseudomonas aeruginosa: utilization of charge, 'specificity determinants,' total hydrophobicity, hydrophobe type and location as design parameters to improve the therapeutic ratio. Chem. Biol. Drug Des. **77**:225–240.
39. **Falla TJ, Karunaratne DN, Hancock RE.** 1996. Mode of action of the antimicrobial peptide indolicidin. J. Biol. Chem. **271**:19298–19303.
40. **Schibli DJ, Nguyen LT, Kernaghan SD, Rekdal O, Vogel HJ.** 2006. Structure-function analysis of tritrpticin analogs: potential relationships between antimicrobial activities, model membrane interactions, and their micelle-bound NMR structures. Biophys. J. **91**:4413–4426.
41. **Mangoni ML, Epand RF, Rosenfeld Y, Peleg A, Barra D, Epand RM, Shai Y.** 2008. Lipopolysaccharide, a key molecule involved in the synergism between temporins in inhibiting bacterial growth and in endotoxin neutralization. J. Biol. Chem. **283**:22907–22917.
42. **Staubitz P, Peschel A, Nieuwenhuizen WF, Otto M, Gotz F, Jung G, Jack RW.** 2001. Structure-function relationships in the tryptophan-rich, antimicrobial peptide indolicidin. J. Pept. Sci. **7**:552–564.
43. **Falla TJ, Hancock RE.** 1997. Improved activity of a synthetic indolicidin analog. Antimicrob. Agents Chemother. **41**:771–775.
44. **Javadpour MM, Barkley MD.** 1997. Self-assembly of designed antimicrobial peptides in solution and micelles. Biochemistry **36**:9540–9549.
45. **Scott MG, Vreugdenhil AC, Buurman WA, Hancock RE, Gold MR.** 2000. Cutting edge: cationic antimicrobial peptides block the binding of lipopolysaccharide (LPS) to LPS binding protein. J. Immunol. **164**:549–553.
46. **Rosenfeld Y, Papo N, Shai Y.** 2006. Endotoxin (lipopolysaccharide) neutralization by innate immunity host-defense peptides. Peptide properties and plausible modes of action. J. Biol. Chem. **281**:1636–1643.
47. **Rosenfeld Y, Shai Y.** 2006. Lipopolysaccharide (endotoxin)-host defense antibacterial peptides interactions: role in bacterial resistance and prevention of sepsis. Biochim. Biophys. Acta **1758**:1513–1522.
48. **Sasaki H, White SH.** 2008. Aggregation behavior of an ultra-pure lipopolysaccharide that stimulates TLR-4 receptors. Biophys. J. **95**:986–993.
49. **Simons RK, Junger WG, Loomis WH, Hoyt DB.** 1996. Acute lung injury in endotoxemic rats is associated with sustained circulating IL-6 levels and intrapulmonary CINC activity and neutrophil recruitment—role of circulating TNF-alpha and IL-beta? Shock **6**:39–45.
50. **Andreasen AS, Krabbe KS, Krogh-Madsen R, Taudorf S, Pedersen BK, Moller K.** 2008. Human endotoxemia as a model of systemic inflammation. Curr. Med. Chem. **15**:1697–1705.